ISSN: 2277-3754
ISO 9001:2008 Certified
International Journal of Engineering and Innovative Technology (IJEIT)
Volume 3, Issue 3, September 2013

An Automatic Delaunay Triangular Mesh Generation Method based On Point Spacing

Lu Sun[1,2,¥] Gour-Tsyh Yeh[1,*] Fang-Pang Lin[3,†] Guoqun Zhao[2,§]
[1] Graduate Institute of Applied Geology, National Central University, Taiwan
[2] Engineering Research Center for Mould & Die Technologies, Shandong University, China
[3]Data Computing Division, National Center for High-Performance Computing, Taiwan

Abstract*—This paper presents a density-controlled Delaunay triangulation system for finite element discretizations of practical engineering problems and scientifically interacting mechanisms. B-splines are constructed to produce boundary points on the curved boundaries of the geometry according to the required point spacing. The lost boundaries in concave and thin geometric features are recovered through recursively inserting pseudo-points on the lost edges. The determinant criterion and modes for removing pseudo-points are correspondingly established as well. Two methods are employed to add interior points: direct method and pre-test method. For the geometry with several sub-domains, corresponding measures for handling overlapped edges are established to ensure the mesh compatibility and element distribution between adjacent sub-domains.

***Index Terms*—Boundary integrity, Delaunay, Point spacing, Voronoi.**

I. INTRODUCTION

Finite element method is a general purpose method for numerical analysis in engineering applications and scientific investigations. It is an important component of computer-aided design and manufacture, and extensively applied in the fields of hydraulics, hydrology, water resources, geotechnical engineering, solid/fluid mechanics, computer graphics, mechanics, and architecture [1], etc. The major characteristic of finite element method is geometry discretion and slice interpolation, i.e. finite element mesh generation. In two-dimensional case, finite element mesh contains two types, triangular mesh and quadrilateral mesh. Among the numerous kinds of triangular mesh generation methods, Delaunay triangulation method is the most widely used one. Delaunay criterion was first proposed by the Russian mathematician, Delaunay [2], in 1934. However, it was not until the early 1980s that Delaunay triangulation method was proposed by Lawson [3] and Watson [4]. Delaunay triangulation method has two crucial criteria: maximum-minimum angle criterion and in-circle criterion. The maximum-minimum angle criterion [5] refers to that the sum of minimal internal angles of all the triangles obtains the maximal value and that of maximal internal angles obtains the minimal value. This criterion enables Delaunay triangulation to automatically avoid generating long and thin elements with small internal angles in two-dimensional case. It not only can guarantee the convergence of the computation, but also ensure that the meshing result is optimal. The in-circle criterion signifies that the circumcircle of each triangle during Delaunay triangulation does not contain any other points. Bowyer-Watson algorithm [4], [6] just takes advantage of the in-circle criterion. Delaunay triangulation algorithm has excellent flexibility and extensibility. It is easily extended to three-dimensional case, so it has attracted many research scholars [7]–[9]. The conventional Delaunay triangulation technique has been relatively mature. The recent research mainly focused on the boundary integrity algorithm of constrained Delaunay triangulation [10], [11], as well as how to overcome the thin elements derived from the degeneration phenomenon of Bowyer-Watson approach. Since the Delaunay triangulation method expresses sufficient effectiveness only for convex geometric features but cannot ensure the boundary integrity for concave features, it is necessary to introduce a boundary recovery procedure when performing Delaunay triangulation to concave domains. This paper adopted Delaunay triangulation method to generate two-dimensional triangular element meshes and developed an automatic triangle meshing system based on point spacing. An intensive study was made on the insertion of boundary points and interior points, boundary integrity, and treatment of overlapped boundaries for multi-domain geometries. Here, the main research content of this paper would be illustrated in detail in the following sections.

II. THEORETICAL FOUNDATION

A. The Voronoi diagram

The implementation of Delaunay triangulation completely relies on the Voronoi diagram. The concept of Voronoi was discovered by the Russian mathematician, Voronoi, in 1908. Suppose given a set of points S in a plane, including n distinct points. For each point P_i, its Voronoi territory, $V(P_i)$, is defined as the locus of points in the plane whose distance to P_i is closer than to any other points of S.

$$V(P_i)=\left\{P / d(P,P_i)\le d(P,P_j)\right\},\ P_i,P_j\in S, j\ne i \qquad (1)$$

The Voronoi cell of each point in S can be expressed as a convex polygon. Thus, the whole plane where *S* is located is divided into n Voronoi polygons, each of which is associated with a unique point in the set. The *n* convex polygons form the Voronoi diagram of point set S. In the

ISSN: 2277-3754
ISO 9001:2008 Certified
International Journal of Engineering and Innovative Technology (IJEIT)
Volume 3, Issue 3, September 2013

Voronoi diagram, every vertex is the common intersection of three edges [6]. The edge of Voronoi polygon is defined as the perpendicular bisector of the line segment joining two adjacent points. When point P_i lies on the boundary of the convex hull, its Voronoi polygon is unbounded. The straight line duality of the Voronoi diagram forms Delaunay triangles [2]. Each Voronoi vertex corresponds to a unique Delaunay triangle and vice versa. For every Voronoi vertex, the circumcircle contains no other points of set S.

B. B-splines

B-spline is short for basis spline, first proposed by Schoenberg [12]. In this paper, B-splines are used to interpolate boundary points for the geometries with curved boundaries.

Assume $\mathbf{P}(u)$ represents the position vector of an arbitrary point in a curved boundary. Then, the k-th order B-spline along variable u is defined by

$$\mathbf{P}(u)=\sum_{i=0}^{n}\mathbf{B}_i N_{i,k}(u) \tag{2}$$

where $\mathbf{B}_i$ indicates the position vectors of the control points, with the number equal to the original points, $n+1$. $N_{i,k}(u)$ denotes the normalized B-spline blending functions. While a k-th order B-spline is constructed, the Cox-de Boor formula [13], [14] of the i-th blending function, $N_{i,k}(u)$, is defined as

$$N_{i,1}(u)=\begin{cases}1 & u\in[u_i,u_{i+1})\\ 0 & \text{otherwise}\end{cases} \tag{3}$$

$$N_{i,k}(u)=\frac{u-u_i}{u_{i+k-1}-u_i}N_{i,k-1}(u)+\frac{u_{i+k}-u}{u_{i+k}-u_{i+1}}N_{i+1,k-1}(u) \tag{4}$$

where u_i represents the knots of the B-spline, with $u_i \le u_{i+1}$.

III. THE IMPLEMENTATION PROCEDURES AND KEY TECHNIQUES OF DELAUNAY TRIANGULATION

Fig. 1 shows the whole implementation process of the triangle meshing system developed in this paper. In the following, the procedures of Voronoi diagram construction and Delaunay triangulation are introduced concretely by taking the geometry shown in Fig. 2(a) as an example.

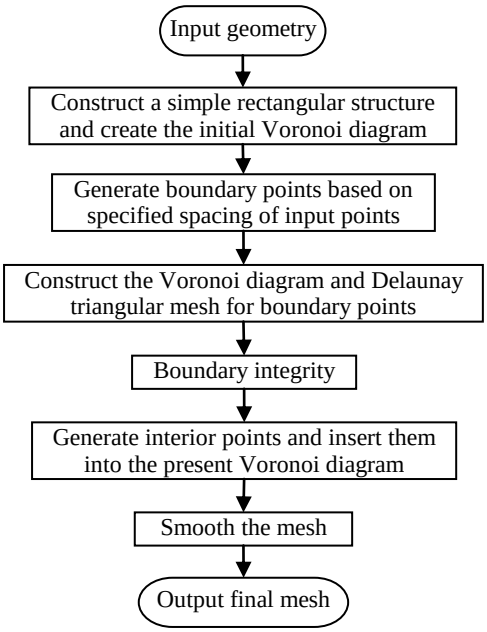

Fig. 1. The procedures of Delaunay triangulation

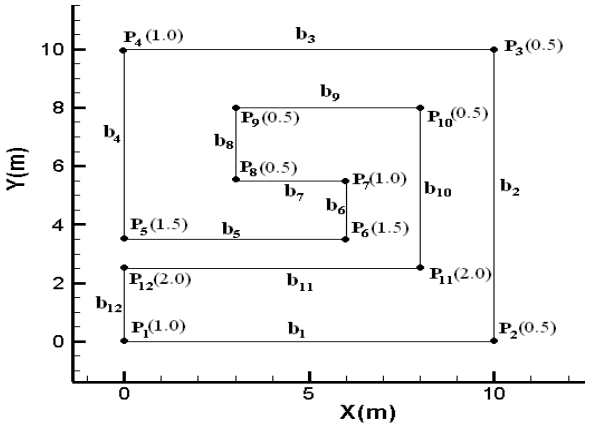

(a) The input data of the geometry

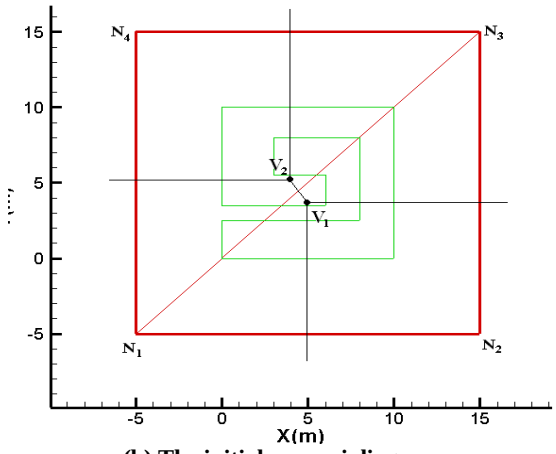

(b) The initial voronoi diagram

ISSN: 2277-3754
ISO 9001:2008 Certified
International Journal of Engineering and Innovative Technology (IJEIT)
Volume 3, Issue 3, September 2013

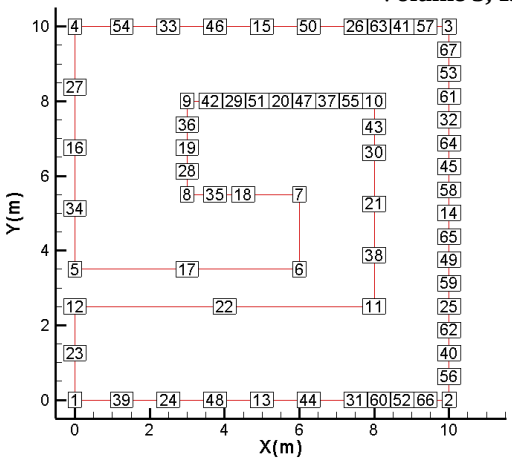

(c) Identification of boundary nodes

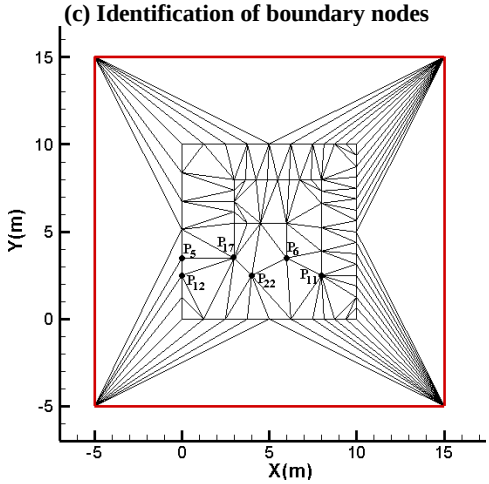

(d) Mesh after inserting boundary nodes

Fig. 2. The generation of boundary points

A. Input data

The meshing system developed in this paper requires two aspects of input data: data points and boundary edges. For the geometry in Fig. 2(a), there are 12 data points, denoted as P_1, P_2 … P_{12}, with the number $np = 12$. The decimal in the parentheses after the point label represents the point spacing specified by users. The geometry consists of 12 boundary edges b_1, b_2 … b_{12}, with the number $nb = 12$. It should be noticed that the input boundary edges for each meshed region must follow such a rule: the outer edges are arranged in counterclockwise order and the inner edges are arranged in clockwise order.

B. Construction of initial Voronoi diagram and Delaunay triangles

First of all, it needs to define a convex hull within which all the input points lie. In this paper, a rectangle enveloping all input points is defined, as seen in Fig. 2(b).

Table I. Data structures of the initial Voronoi diagram

Voronoi	Forming points			Neighboring Voronoi		
	1	2	3	1	2	3
V_1	N_1	N_2	N_3	none	V_2	none
V_2	N_1	N_3	N_4	none	none	V_1

Then, construct the initial Voronoi diagram and Delaunay triangular elements based on the rectangular structure. The initial diagram is composed of two Voronoi vertices (V_1 and V_2) and two Delaunay triangles. Table I lists the data structures of the initial diagram [6], [7].

C. Generation of boundary points according to specified point spacing

Before boundary-point creation, it needs to subdivide the geometry boundaries into several segments. To achieve correct subdivision, special corner points are suggested to be identified first. A special corner point is defined as the point where three or more boundary edges meet. This paper established the segmentation rule as follows: (1) the straight edge is considered as a single segment itself; (2) the end-to-end curved edges are integrated to form a whole segment; (3) if a special corner point is encountered, its connected edges are regarded as belonging to different segments. The boundary points are generated based on the specified point spacing. The point spacing is reflected by the lengths of the edges connected to the point. Taking the i-th edge b_i as an example, suppose that the two endpoints of b_i are P_a and P_b with specified point spacing labeled as $ps(P_a)$ and $ps(P_b)$, respectively.

First, compute the midpoint of b_i, denoted as P_m. If b_i belongs to a curved segment, B-spline should be created. P_m is identified as the point derived from interpolation at $u_m = (u_a + u_b)/2$ by "(2)", "(3)", and "(4)". Then, compute the practical point spacing at P_m by

$$ps'(P_m) = \left(|P_aP_m| + |P_mP_b|\right)/2 \qquad (5)$$

Second, check whether P_m is required to be inserted. Determine the lower value between $ps(P_a)$ and $ps(P_b)$, denoted as $ps(\min)$. If $ps'(P_m)$ is larger than $ps(\min)$, accept P_m. Otherwise, reject P_m and turn to the check for the next edge. If P_m is accepted, update the data information of relevant points and edges. And, a specified point spacing value is assigned to P_m by interpolation.

$$ps(P_m) = \alpha \frac{ps(P_a)|P_mP_b| + ps(P_b)|P_aP_m|}{|P_aP_m| + |P_mP_b|} \qquad (6)$$

At the same time, edge b_i is decomposed into two new edges. Then, the above procedures are repeated over the two new edges again until the practical point spacing are able to satisfy the specified values. Fig. 2(c) provides the boundary contour after identifying the inserted points based on specified point spacing, containing 67 points and 67 edges. The numbers in

ISSN: 2277-3754
ISO 9001:2008 Certified
International Journal of Engineering and Innovative Technology (IJEIT)
Volume 3, Issue 3, September 2013

square boxes represent the serial numbers of the boundary points.

D. Construction of Voronoi diagram and Delaunay triangles of boundary points

Now, we insert all the boundary points into the initial Voronoi diagram. Taking the point set in Fig. 3(a) as the example, suppose that there are 11 distinct points in set S, P_1, P_2, P_3 ... P_{11}, and a new point P_{12} will be inserted to the present Voronoi diagram. The insertion operation is realized through the following steps [6]:

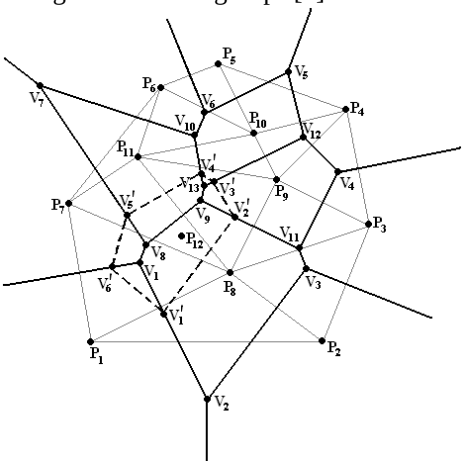

(a) the original Voronoi diagram

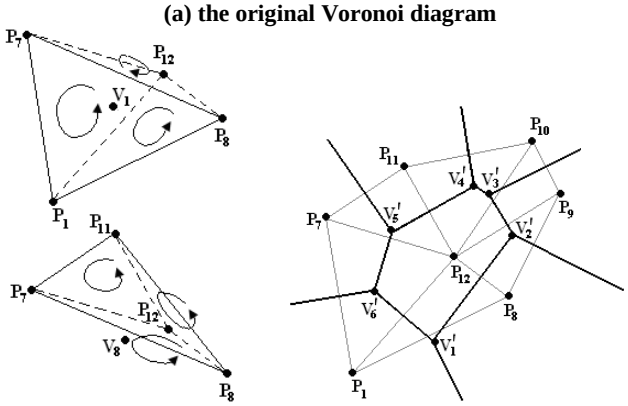

(b) Check position relationships (c) local Voronoi diagram Of point and triangle

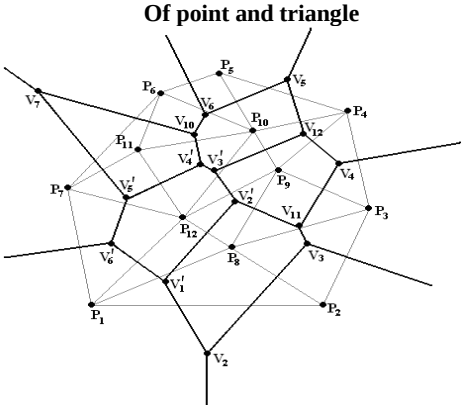

(d) Global Voronoi diagram

Fig. 3. Insertion of new point

(1) Identify the Delaunay triangle and the Voronoi structure containing the new point. To save computing time and reduce programming work, this paper uses the right-hand rule to check the position relationships between the new point and each Delaunay triangle. For an arbitrary Delaunay triangle, say randomly selected, the introduced point is able to form three new triangles with its three edges. For example, the introduced point P_{12} divides the Delaunay triangle $P_1P_8P_7$ (corresponding to Voronoi vertex V_1, this triangle is selected randomly on the first try) into three new smaller ones, as the amplified view shown in Fig. 3(b). Then, the right-hand rule is employed to check whether these three triangles have the same rotations. The check result shows that the orientations of triangles $P_{12}P_1P_8$ and $P_{12}P_7P_1$ are both counterclockwise, whereas that of triangle $P_{12}P_8P_7$ is different. So, Point P_{12} is in the exterior of triangle $P_1P_8P_7$ and is located in the outside of the edge P_8-P_7. In order to save time, the follow-up search process is performed from the vertices adjacent to V_1 (corresponding to triangle $P_1P_8P_7$) and in the outer side of edge P_8-P_7. Then, Voronoi vertex V_8 and its duality Delaunay triangle $P_7P_8P_{11}$ are selected for check. As shown in Fig. 3(b), new point P_{12} forms three new triangles with the three edges of triangle $P_7P_8P_{11}$. According to right-hand rule, these three new triangles have the same rotations of counterclockwise. Therefore, the dual Delaunay triangle of Voronoi Vertex V_8 is just the triangle containing point P_{12}.

(2) Determine the Voronoi vertices to be deleted.

According to the fundamental property of Voronoi diagram that the circumcircle of each vertex only contains its three forming points but not involves any other points, the vertices whose circumcircles contain the newly inserted point should be deleted. As shown in Fig. 3(a), there are four Voronoi vertices to be deleted, V_1, V_8, V_9, and V_{13}. Their dual Delaunay triangles should be deleted as well.

(3) Construct local Voronoi diagram and Delaunay triangles

When the identified vertices are deleted, an empty convex polygon arises in the deleted region, as the polygon $P_1P_8P_9P_{10}P_{11}P_7$ shown in Fig. 3(a). The new point P_{12} is in the interior of the polygon. The edges P_1-P_8, P_8-P_9, P_9-P_{10}, P_{10}-P_{11}, P_{11}-P_7, and P_7-P_1 of the empty polygon are the residual edges of deleted triangles in practice. Every residual edge gives rise to a new Voronoi vertex with P_{12}. In this case, six new vertices are constructed, as V_1', V_2', V_3', V_4', V_5', and V_6' shown in Fig. 3(c).

(4) Merge the local Voronoi diagram into the global diagram

The merger of local Voronoi diagram contains two aspects. The first is to add the newly generated vertices to the original diagram directly. The second is to modify some of the

ISSN: 2277-3754
ISO 9001:2008 Certified
International Journal of Engineering and Innovative Technology (IJEIT)
Volume 3, Issue 3, September 2013

neighboring information of the Voronoi vertices adjacent to the deleted vertices. Fig. 3(d) shows the new Voronoi diagram after inserting point P_{12}.

(5) After one point is inserted, repeat above steps (1)-(4) to insert the next one.

For the geometry in Fig. 2(a), the 67 boundary points (see Fig. 2(c)) are inserted into the initial Voronoi diagram (see Fig. 2(b)) by the method stated above. And, the Delaunay triangles formed by all boundary points are achieved, as shown in Fig. 2(d).

E. Boundary integrity

Make an intuitive comparison of the boundary contours between the input geometry in Fig. 2(a) and the mesh after inserting boundary points in Fig. 2(d). It is clearly seen that the input edges b_5 and b_{11} are missing. This is an inevitable issue when performing Delaunay triangulation for a given set of boundary edges which are defined by their endpoints. It usually occurs in concave or thin features of the geometry because the distance between two input edges is relative small. In this paper, a posteriori method is employed to recover lost boundaries by adding pseudo-points iteratively [7], [8].

1. Add pseudo-points

As shown in Fig. 2(c), after the boundary points are generated according to the specified point spacing, the input edges b_5 and b_{11} have been converted into P_5-P_{17}, P_{17}-P_6 and P_{11}-P_{22}, P_{22}-P_{12}, respectively. And the lost edges in Fig. 2(d) are P_{17}-P_6, P_{11}-P_{22}, and P_{22}-P_{12} in practice.

Pseudo-points are produced at the midpoints of the lost edges. For example, pseudo-point P_{69} is added at the midpoint of edge P_{17}-P_6. Following by that, new Voronoi diagram is established. Edge P_{17}-P_6 is subdivided into P_{17}-P_{69} and P_{69}-P_6. For each new edge, further check continues until there is no missing edge left.

Fig. 4(a) shows the triangular mesh after adding pseudo-points, where black points P_{68}, P_{69}, and P_{70} represent the added pseudo-points. Fig. 4(b) shows the resulting mesh after eliminating the Voronoi vertices outside the geometry.

2. Removal of pseudo-points

The addition of pseudo-points resolves the boundary loss problem successfully, but also has a serious impact on the accurate control of mesh density. Since the pseudo-point is added at the midpoint of the lost edge, the accuracy of geometric description for curved boundaries is decreased to some extent. To resolve this problem, the added pseudo-points should be removed again under the premise of holding the integrity of geometry boundaries. In this paper, several removal modes of pseudo-points are established by defining different contracted points. Fig. 5 provides the establishment of removal modes by taking the pseudo-point P_{69} as the example.

First of all, the Voronoi vertices whose dual Delaunay triangles share the pseudo-point should be found out. The four triangles sharing P_{69} are $P_{69}P_{35}P_{17}$, $P_{69}P_{18}P_{35}$, $P_{69}P_7P_{18}$, and $P_{69}P_6P_7$ as in Fig. 5(a).

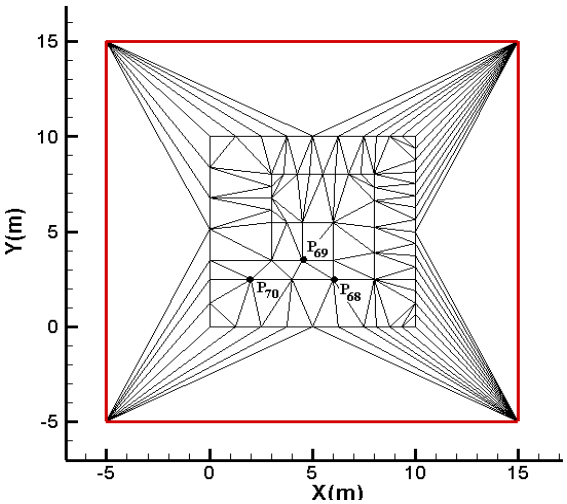

(a) Add pseudo-points

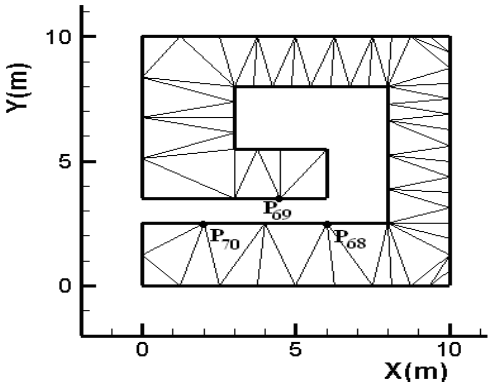

(b) Delete outside vertices

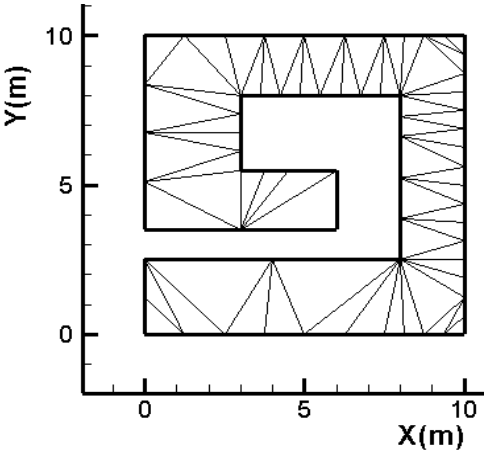

(c) Remove pseudo-point

Fig. 4. Boundary integrity

ISSN: 2277-3754
ISO 9001:2008 Certified
International Journal of Engineering and Innovative Technology (IJEIT)
Volume 3, Issue 3, September 2013

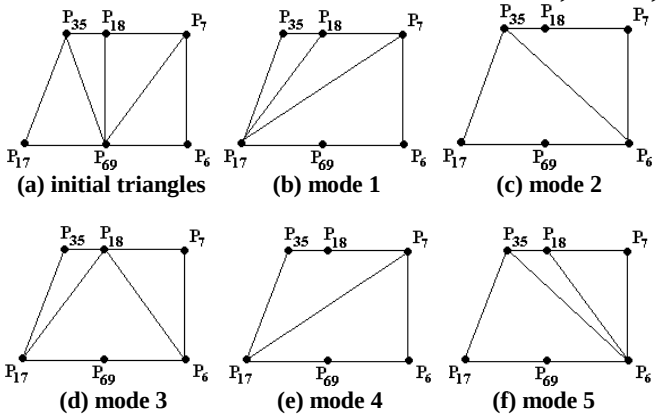

Fig. 5. Pseudo-point removal

Table II. Point structures of each removal mode

Voronoi	Mode 1	Mode 2	Mode 3	Mode 4	Mode 5
V_1	P_{17}, P_6, P_7	P_{35}, P_{17}, P_6	P_{18}, P_{35}, P_{17}	P_7, P_{18}, P_{35}	P_6, P_7, P_{18}
V_2	P_{17}, P_7, P_{18}	P_{35}, P_6, P_7	P_{18}, P_{17}, P_6	P_7, P_{35}, P_{17}	P_6, P_{18}, P_{35}
V_3	P_{17}, P_{18}, P_{35}	P_{35}, P_7, P_{18}	P_{18}, P_6, P_7	P_7, P_{17}, P_6	P_6, P_{35}, P_{17}

Then, choose a contracted point from the forming points of the Voronoi vertices connected to the pseudo-point. In principle, every forming point of the triangles except the pseudo-point to be removed can be considered as a contracted point. Each of the original triangles provides an edge to form a new triangle with the contracted point. In this case, five removal modes can be established for the situation of Fig. 5(a) respectively by taking point P_{17}, P_{35}, P_{18}, P_7, and P_6 as the contracting point, as shown in Fig. 5(b)-(f). The point structures of the Voronoi vertices for these five removal modes are listed in Table II. It can be seen that no matter which mode is applied, the original four Voronoi vertices will always be reduced to three ones. The next step is to select the most reasonable removal way from the five modes in Fig. 5(b)-(f). This paper employs two judgment criteria to realize the selection operation: *Jacobian* and minimum angle.

(1) The *Jacobian*

The *Jacobian* matrix [15] is the basic indicator to reflect mesh quality. Fig. 6(a) shows a triangle with three forming points denoted as $P_1(x_1, y_1)$, $P_2(x_2, y_2)$, and $P_3(x_3, y_3)$ ordered in the counterclockwise direction. At each point P_i, the *Jacobian* matrix is expressed as:

$$\mathrm{A} = \begin{pmatrix} x_i - x_k & y_i - y_k \\ x_j - x_i & y_j - y_i \end{pmatrix} \tag{7}$$

$$Jacobian = \det(\mathrm{A}) \tag{8}$$

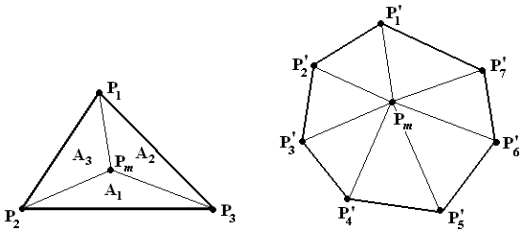

Fig. 6. Insertion of interior point

where $i, j, k = 1, 2, 3$. If $i = 1$, then $j = 2$ and $k = 3$. If $i = 2$, then $j = 3$ and $k = 1$. If $i = 3$, then $j = 1$ and $k = 2$.

For a triangle in two-dimensional space, three *Jacobian* values, one each for one of its three points, can be calculated by "(7)" and "(8)". Among these three *Jacobians*, compute the minimal value as the *Jacobian* of the triangle. If the *Jacobian* of a triangle is larger than zero, it signifies that its orientation is positive and satisfies the requirements of mesh generation. If the *Jacobian* is equal to zero, it signifies that the triangle is degenerated into a single straight-line. If the *Jacobian* is negative, the triangle is distorted or overlapped. Therefore, only the triangles with $Jacobian > 0$ are permitted for a finite element mesh. Compute the *Jacobian* values of the triangles for the five modes in Fig. 5(b)-(f). The result shows that $P_{35}P_7P_{18}$ in mode 2 and $P_7P_{18}P_{35}$ in mode 4 both have $Jacobian \le 0$, which exceeds the acceptable range and is not permitted for a finite element mesh. By *Jacobian* criterion, mode 2 and 4 are excluded. The follow-up work is focused on selecting the best mode from modes 1, 3, and 5.

(2) The minimum angle

The minimum angle is another important indicator for the evaluation of triangular mesh quality. In this paper, the minimum angle of each mode is defined as the minimal value among the minimum angles of all the triangles in that mode.

$$l_{\min} = \min(l_i) \qquad i = 1, 2 \ldots n \tag{9}$$

Compute the minimum angle of each possible mode by "(9)". The one which yields the largest value is selected as the actual way. Computing result shows that the minimum angles of modes 1, 3, and 5 are 16.31^o, 16.31^o, and 11.49^o, respectively. So, exclude mode 5 and accept mode 1 in sequence. Fig. 4(c) shows the resulting mesh after boundary integrity, which can precisely capture the boundary features of the analyzed geometry.

F. Generation of interior points

This paper uses two methods to produce interior points: the direct method and pre-test method.

1. The direct method

The direct method generates the interior points according to the specified point spacing of the points around them

ISSN: 2277-3754
ISO 9001:2008 Certified
International Journal of Engineering and Innovative Technology (IJEIT)
Volume 3, Issue 3, September 2013

directly. As shown in Fig. 6(a), an interior triangle has three forming points labeled as P_1, P_2, and P_3, its interior point can be computed by four steps:

(1) Compute the centroid of the triangle, labeled as P_m.

(2) Compute the practical point spacing at P_m by interpolation.

$$ps'(P_m) = \beta \frac{\sum_{i=1}^{3} (|P_m P_i| A_i)}{\sum_{i=1}^{3} A_i} \qquad i = 1,2,3 \qquad (10)$$

where β is an adjust parameter ranging from 0.5 to 1.0 and A_i represents the area of the triangle formed by P_m and another two points, as shown in Fig. 6(a).

(3) Determine the minimal value of $ps(P_1)$, $ps(P_2)$, and $ps(P_3)$, denoted as $ps(\min)$. $ps(\min)$ is considered as the required point spacing at P_m.

(4) Check whether $ps'(P_m)$ is larger than $ps(\min)$. If yes, accept P_m. If no, reject P_m. If P_m is accepted, insert it into the present Voronoi diagram. At the same time, a point spacing value, $ps(P_m)$, is assigned by interpolation.

$$ps(P_m) = \frac{\sum_{i=1}^{3} (A_i ps(P_i))}{\sum_{i=1}^{3} A_i} \qquad i = 1,2,3 \qquad (11)$$

2. Pre-test method

Pre-test method generates interior points through a previous test process. For the triangle of Fig. 6(a), pre-test method is performed by the following steps:

(1) Compute the centroid of the triangle, P_m.

(2) Suppose that P_m is required for generation. Insert it to the present Voronoi diagram, delete the Voronoi vertices whose circumcirles contain P_m and construct an empty polygon, see Fig. 6(b), where P_i' denotes the points on the empty polygon.

First, compute the practical point spacing of P_m by

$$ps'(P_m) = \frac{1}{n} \sum_{i=1}^{n} |P_m P_i'| \qquad (12)$$

Then, pick out the minimum value of the specified point spacing among the n points P_i', denoted as $ps(\min)$.

Compare the values of $ps'(P_m)$ and $ps(\min)$. If $ps'(P_m) > ps(\min)$, accept P_m to reduce the error. Otherwise, reject P_m. If P_m is accepted, insert it into the present Voronoi diagram and assign a point spacing as its specified value during the subsequent procedures.

$$ps(P_m) = \frac{1}{n} \sum_{i=1}^{n} ps(P_i') \qquad (13)$$

3. The control on the number of cycles for inserting interior points

When the interior points are inserted into a triangle lying on the geometry boundaries, some undesired problems might be considered. If a triangle has two points on the boundaries with larger values of specified point spacing and one point in the interior with a relatively smaller value of specified point spacing, the practical point spacing at the centroid may be increased undesirably due to the long length of boundary edge. This will result in the ceaseless insertion of interior points and thereby reducing the quality of boundary triangles, and even leads to an endless loop of programming and the non-convergence of solution. In order to avoid that problem, a termination condition for the cycle control on inserting interior points is employed, that is, the radius radio of the circumcircle to the in circle of the triangle. In this paper, if a triangle has the ratio larger than 2.0, it is considered that there is no longer need to insert any interior points to it.

4. Smooth of interior points

Laplacian method [16] is the most commonly used method for point smooth. It moves each point to the average position of its neighboring points or elements in the most simplest and straightforward way. Assume that the original coordinates of an interior point P_i are $P_i(x_0, y_0)$. Its position coordinates after smooth can be calculated by

$$P_i(x,y) = P_i(x_0,y_0) + \mu\left(\frac{1}{n}\sum_{j=1}^{n} C_j(x,y) - P_i(x_0,y_0)\right) \qquad (14)$$

where, $C_j(x,y)$ and n respectively represent the center and the number of the triangles connected to P_i. μ is an adjustment factor and set to 0.8 in this paper. Fig. 7(a) shows the resulting mesh after inserting interior points using direct method, consisting of 152 points and 227 triangles. Fig. 7(b) shows that using pre-test method, with 229 points and 381 triangles. Both of these two meshes can realize the effective control on the density distribution of the points and elements. In comparison with the pre-test method, the direct method occupies less storage space, spends less time and improves the meshing efficiency significantly. Whereas the pre-test method increases the programming work and meshing time due to the operation of previous test. But, when pre-test method is used, the density transition is rather smooth. Fig. 7(c) and (d) provide the final meshes after smooth of the resulting meshes in Fig. 7(a) and (b).

ISSN: 2277-3754
ISO 9001:2008 Certified
International Journal of Engineering and Innovative Technology (IJEIT)
Volume 3, Issue 3, September 2013

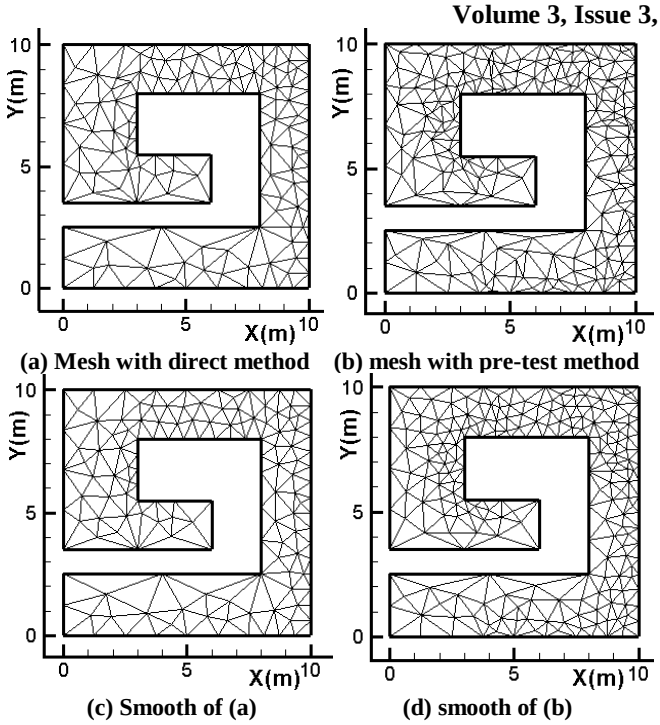

Fig. 7. Insertion and smooth of interior nodes

IV. CONTROL OF MESH DENSITY FOR GEOMETRIES WITH SEVERAL SUB-DOMAINS

In practical engineering applications, it is usually required to generate Delaunay triangular meshes for the geometries with several sub-domains. Such meshes are required to meet the following conditions in general: (1) Different sub-domains have different density distribution; (2) The mesh on the intersecting boundaries of two neighboring sub-domains has to share the common points and edges; (3) The points on the intersecting boundaries are conformal for both of the local meshes of two associated sub-domains; (4) The density transition of two adjacent sub-domains should as smooth as possible. These conditions enhance the difficulty in Delaunay triangulation for multi-domain geometry considerably. In order to ensure the mesh conformity for the geometries with several sub-domains, this paper established the corresponding method and treatment way through identification and treatment of overlapped edges. The edges on the intersecting boundaries are treated as overlapped edges. Special treatment procedures are carried out for the conformity of the boundary points on overlapped edges.

A. Identification of overlapped boundary edges

When the two-dimensional geometric model to be meshed contains several sub-domains, the boundaries for each sub-domain should be input separately. For example, the geometry as shown in Fig. 8(a) has three sub-domains. The boundary edges of the first sub-domain are input as outer ring P_1-P_2-P_3-P_4 and inner ring P_8-P_7-P_6-P_5. The second sub-domain is input as outer ring P_5-P_6-P_7-P_8 and inner ring P_{12}-P_{11}-P_{10}-P_9. The third sub-domain contains only one ring, P_9-P_{10}-P_{11}-P_{12}. First of all, the overlapped boundary edges, i.e. the edges on the intersecting boundaries of two neighboring sub-domains, have to be picked out, as the edges on rings P_5-P_6-P_7-P_8 and P_9-P_{10}-P_{11}-P_{12}.

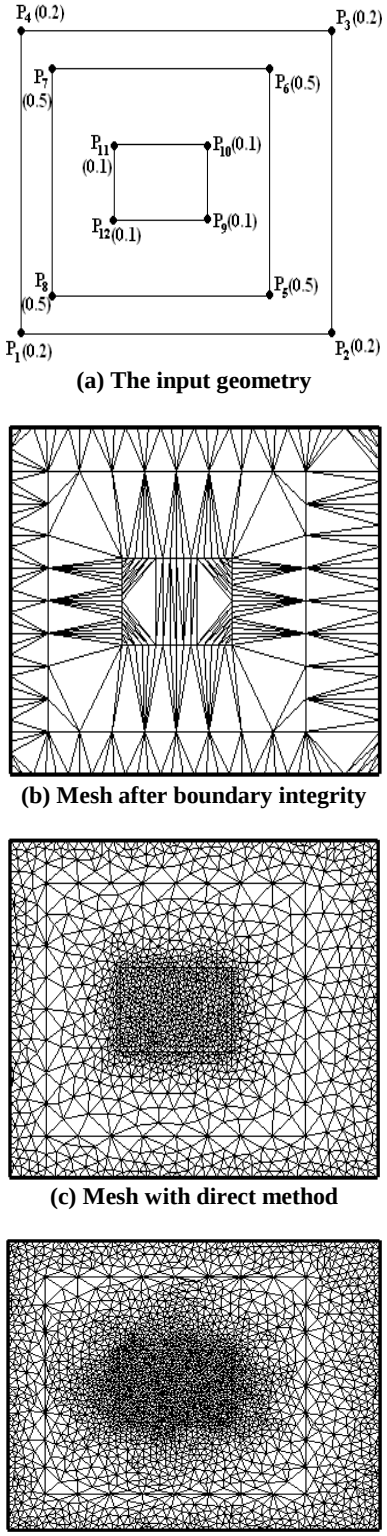

Fig. 8. Treatment of overlapped boundaries for the geometry with several sub-domains

ISSN: 2277-3754
ISO 9001:2008 Certified
International Journal of Engineering and Innovative Technology (IJEIT)
Volume 3, Issue 3, September 2013

B. Treatment of overlapped edges

It should be noticed that the points on the intersecting boundaries are shared by both of the adjacent sub-domains but the edges are overlapped and each belongs to its own sub-domain only. For this reason, in the subsequent meshing procedures, overlapped boundaries have to be treated particularly.

(1) In the process of identification and insertion of boundary points on the overlapped edges based on point spacing, the points are added only once, but the edges are updated repeatedly. For example, P_{15} is added on the pair of overlapped boundary edges P_6-P_5 and P_5-P_6. Once P_{15} is inserted, the pair of overlapped edges P_6-P_5 and P_5-P_6 are divided into two new pairs.

(2) During the process of boundary integrity, the insertion and removal of pseudo-points are performed once but the updating of edges is repeated.

Fig. 8(b) shows the resulting mesh after boundary integrity. Each point on the overlapped edges is unique. But, the overlapped edges are updated with the addition of new points correspondingly. The newly generated edges on the overlapped boundaries are also overlapped. Fig. 8(c) and (d) provide final meshes when direct method and pre-test method are used. In these two meshes, the points on the overlapped boundaries are conformal for their two connected sub-domains.

V. APPLICATIONS

The whole procedures and key techniques of Delaunay triangulation illustrated above are implemented by object-oriented C++ programming. In this section, three examples are provided to demonstrate the reliability and effectiveness of the system developed in this paper. The first example is about a geometrical model containing curved boundaries and two sub-domains, as shown in Fig. 9(a). The thick lines indicate straight boundaries and thin lines indicate curved boundaries. According to the curved and straight status, the geometry boundaries are decomposed into five segments, where S_1, S_3, and S_5 are curved so that B-splines should be constructed for them. Fig. 9(b) shows the boundary contour map of the geometry after generating boundary points. Fig. 9(c) shows the final mesh using direct method, containing 1,151 points and 2,215 triangles. Fig. 9(d) shows the final mesh using pre-test method, with 1,906 points and 3,725 triangles. Fig. 10 presents the second triangle meshing example, containing nine sub-domains and three factors required to be refined particularly: point P_1, edge P_2-P_3, and segment S_1. Segment S_1 is a curved line formed by eight points, and required to construct a smooth curve using B-splines, as shown in Fig. 10(b). In addition, there are a lot of overlapped edges on the intersecting boundaries between each pair of neighboring sub-domains. These overlapped edges require treated specially. Fig. 10(c) shows the final mesh with the interior points generated using direct method, consisting of 2,754 points and 5,430 triangles in all. Fig. 10(d) provides the locally amplified views of the three refinement factors. The third example is to generate triangular mesh for a complicated geometrical model containing a single domain and several curved boundaries, as shown in Fig. 11(a). Fig. 11(b) shows the final mesh, consisting of 5,746 points and 10,908 triangles. Obviously, the triangular meshes generated by the system developed in this paper are able to capture the boundary features of the geometry precisely. The density of mesh elements is distributed reasonably according to the specified point spacing.

VI. CONCLUSION

This paper presented the implementation of Delaunay triangulation to generate high quality meshes with prescribed heterogeneous spacing. The applications proved that our developed system was able to generate high-quality and reasonable-density triangular meshes for input geometries.

(1) Our system generated boundary points by recursively inserting midpoints according the specified point spacing. B-splines were constructed for the curved boundaries. In this way, the reasonable distribution and smooth transition of the points on geometry boundaries were achieved. And the boundary mesh was able to capture the geometric features especially curved features of the analyzed model precisely.

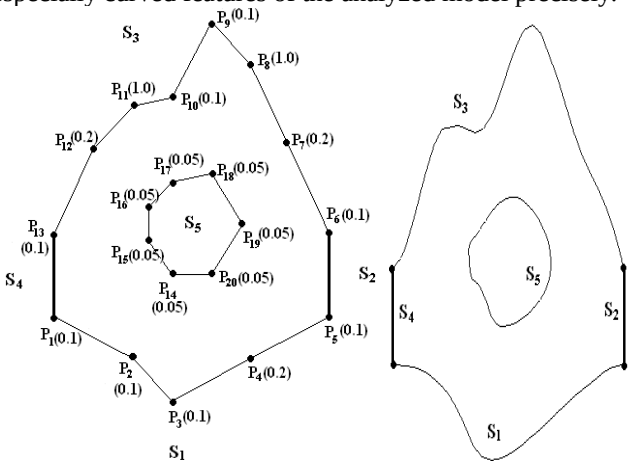

(a) The input geometry **(b) Boundary contour after Generating boundary points**

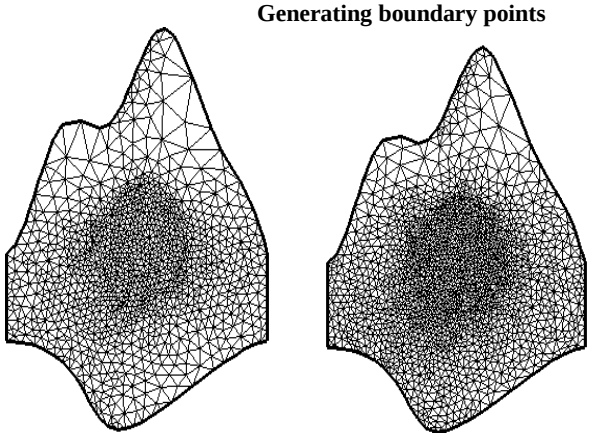

(c) Mesh with direct method **(d) mesh with pre-test method**

Fig. 9. Example 1

ISSN: 2277-3754
ISO 9001:2008 Certified
International Journal of Engineering and Innovative Technology (IJEIT)
Volume 3, Issue 3, September 2013

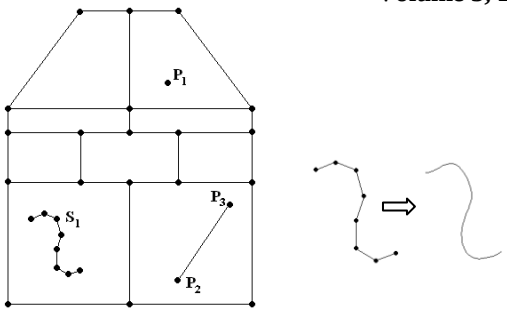

(a) The input geometry (b) construction of B-spline curve

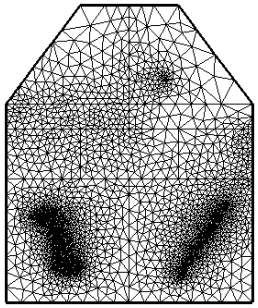

(c) Final mesh

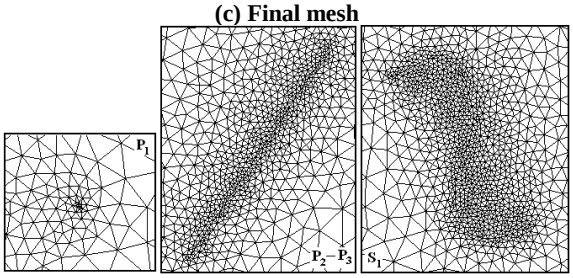

(d) Amplified views of refinement factors

Fig. 10. Example 2

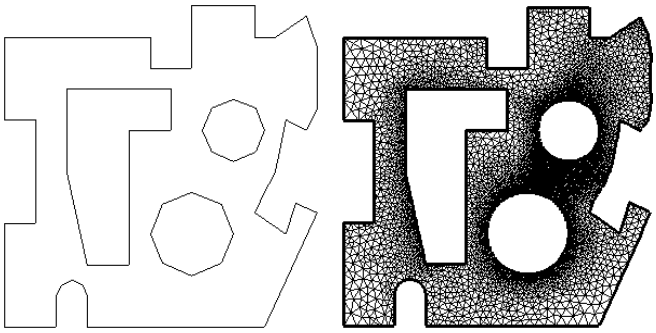

(a) The input geometry (c) final mesh

Fig. 11. Example 3

(2) Our system resolved boundary loss problem by adding pseudo-points. Two criteria for selecting removal modes were employed as well. By using this method, the lost boundaries are recovered successfully. The mesh after boundary integrity can capture the boundary features of the geometry accurately.

(3) Two methods were used to generate interior points: direct method and pre-test method. Laplacian method was used to smooth the interior points. The proper distribution and conformal transition of interior points was realized effectively.

(4) For the geometries with several sub-domains, overlapped boundary edges were established. Corresponding methods were established to treat the overlapped boundaries. The reasonable distribution and excellent conformity of the triangles and points between adjacent sub-domains are implemented correctly.

VII. ACKNOWLEDGMENT

This research is supported, in part, by National Science Council under contract Nos. NSC 101-2116-M-008-002 and NSC 101-2811-M-008-067 with National Central University and, in part, by National Central University under the 5/500 Fund.

REFERENCES

[1] O. C. Zienkiewicz, "Achievements and some unsolved problems of the finite element method," International Journal for Numerical Methods in Engineering, vol. 47, pp. 9-28, Jan. 2000.

[2] B. Delaunay, "Sur la sphere vide," Bulletin of Academy of Sciences of the USSR, vol. 7, pp. 793-800, 1934.

[3] C. L. Lawson, "Software for C1 surface interpolation," in: Mathematical Software III, J. R. Rice (ed)., Academic Press, New York, pp. 161-194, 1977.

[4] D. Watson, "Computing the n-dimensional Delaunay tessellation with applications to Voronoi polytopes," The Computer Journal, vol. 24, pp. 167-172, 1981.

[5] R. Sibson, "Locally equiangular triangulations," The Computer Journal, vol. 21, pp. 243-245, 1978.

[6] A. Bowyer, "Computing Dirichlet tessellations," The Computer Journal, vol. 24, pp. 162-166, Jan. 1981.

[7] N. P. Weather ill, "Delaunay triangulation in Computational Fluid Dynamics," Computers & Mathematics with Applications, vol. 24, pp. 129-150, Sep. 1992.

[8] N. P. Weather ill, "The integrity of geometrical boundaries in the two-dimensional Delaunay triangulation," Communications in Applied Numerical Methods, vol. 6, pp. 101-109, Feb. 1991.

[9] J. R. Shewchuk, "Delaunay refinement algorithms for triangular mesh generation," Computational Geometry-Theory and Applications, vol. 22, pp. 21-74, May 2002.

[10] P. L. George, F. Hecht, and E. Saltel, "Automatic mesh generator with specified boundary," Computer Methods in Applied Mechanics and Engineering, vol. 92, pp. 269-288, Nov. 1991.

[11] P. L. George and H. Borouchaki, "Delaunay Triangulation and Meshing: Application to Finite Elements," Paris, Editions HERM ES, 1998.

[12] I. J. Schoenberg, "Contributions to the problem of approximation of equidistant data by analytic functions, Part A: On the problem of smoothing of graduation, a first class of analytic approximation," Quarterly of Applied Mathematics, vol. 4, pp. 45-99, 1946.

[13] C. De Boor, "On calculating with B-splines," Journal of Approximation theory, vol. 6, pp. 50-62, 1972.

[14] M. G. Cox, "The numerical evaluation of B-splines," IMA Journal of Applied Mathematics, vol. 10, pp. 134-149, 1972.

ISSN: 2277-3754
ISO 9001:2008 Certified
International Journal of Engineering and Innovative Technology (IJEIT)
Volume 3, Issue 3, September 2013

[15] P. M. Knupp, "A method for hexahedral mesh shape optimization," International Journal for Numerical Methods in Engineering, vol. 58, pp. 319-332, Sep. 2003.

[16] D. A. Field, "Laplacian smoothing and Delaunay triangulations," Communications in Applied Numerical Methods, vol. 4, pp. 709-712, 1988.

AUTHOR'S PROFILE

Correspondent author: Gour-Tsyh Yeh

Education:

1967 – 1969: Ph.D. Hydrology, Cornell University
1966 – 1967: M.S. Hydraulics, Syracuse University
1960 – 1964: B.S. Civil Engineering, National Taiwan University

Research area:

Hydrology, environmental fluid mechanics, hydraulics, and water resources, physics-based first principle approaches of watershed modeling, coupled surface and subsurface flow and transport processes, geochemical kinetics, biodegradation and micro-organism/geochemical interactions, geochemical equilibrium modeling, multi-phase flow and transport in both fractured and porous media, development of innovative numerical algorithms, and computational fluid dynamics.

Experience:

2010-Date NSC Chair Professor, Graduate Institute of Applied Geology, National Central University, Jhongli, Taoyuan, Taiwan
2000-2010 Provost Professor, Department of Civil and Environmental Engineering, University of Central Florida, Orlando, FL.
1989-2000 Professor, Department of Civil and Environ. Eng., Pennsylvania State University, University Park, PA
1977-1989 Senior Research Staff (1983-1989); Research Staff II (1977-1983) Oak Ridge National Laboratory, Oak Ridge, TN
1973-1977 Senior Hydraulic Engineer (1973-1975); Senior Environmental Engineer (1976-1977), Stone and Webster Engineering Corporation, Boston, Massachusetts
1975-1976 Senior Engineer Tetra Tech, Inc., Pasadena, California.
1972-1973 Senior Engineer, Ebasco Services, Inc., New York, New York.
1971-1972 Visiting Scientist on NRC Research Associateship, NASA, Houston, Texas
1971-1971 Visiting Associate Professor, Dept. of Civil Engineering, National Taiwan University, Taipei, Taiwan
1969-1971 Research Associate, Dept. of Civil Engineering, Cornell University, Ithaca, New York
1967-1969 Research Assistant Dept. of Civil Engineering, Cornell University, Ithaca, New York
1966-1967 Research Assistant, Dept. of Civil Engineering, Syracuse University, Syracuse, New York

Achievements:

(1) Published two books and more than 400 papers, technical reports, and conference proceedings; highest citation=435; Number of publications with over 100 citation = 7; H-Index = 26.
(2) Developed over 100 physics-based process-level computational models: many of which has been adopted as the de facto standard by academic communities, federal agencies, and industries
(3) Conducted more than 40 interdisciplinary research projects with a total funding of over $8,000,000
(4) Received Presidential PIP Award, Martin Marietta Publication Award, NRC Research Associateship, NRC Senior Research Associateship, PSES Outstanding Research Award, UCF Distinguished Researcher, UCF Graduate Teaching Award, NTU Outstanding Alumni
(5) Consultant, IAEA, Unite Nations
(6) Completed over 40 consulting jobs for over 30 clients
(7) Offered short courses, seminars, and workshops many times on subsurface flow and reactive chemical transport
(8) Organized and chaired more than 10 salient national and international symposia
(9) Advised and supervised over 25 Ph.D. and M.S. students at University of Central Florida and Penn State in 21 years

First author: Lu Sun

2012-Date Post-doctoral researcher, Graduate Institute of Applied Geology, National Central University, Taiwan
2008-2012 Ph.D. Materials Science and Engineering, Shandong University, China
2006-2008 M.S. Materials Science and Engineering, Shandong University, China
2002-2006 B.S. Materials Science and Engineering, Shandong University, China

Research area:

Finite element mesh generation

Third author: Fang-Pang Lin

Education:

1991-1995 Ph.D. Department of Civil Engineering, University of Swansea Wales
1990 -1991 M.S. Department of Civil Engineering, University of Swansea, Wales
1984 -1987 B.S. Department of Civil Engineering, National Chiao-Tung University

Research area:

Computational Fluid Dynamics, Finite Element Analysis, Multigrid Methods, Parallel and Distributed Computing, Optimization Design, and Grid Computing

Working Experiences:

2003-Date Research Scientist, Division Manager, Grid Computing Division, NCHC, Taiwan
2000- 2002 Associate Research Scientist, Software Development Division, NCHC, Taiwan
1996-1997 Visiting Research Scientist, Oxford University Computing Laboratory, UK
1995-1996 Postdoctoral research, Department of Civil Engineering, University of Swansea Wales, UK

Achievements:

(1) Published published more than 40 papers and reports.
(2) Received the highest technology development award by Executive Yuan, Republic of China (Taiwan)
(3) Organized and chaired more than 20 international conferences
(4) Deputy Chair, PRAGMA (Pacific Rim Applications and Grid Middleware Assembly) Steering Committee; Steering Committee Member, RCN (Research Coordination Network); Steering Committee Member, GLEON (Global Lake Environmental Observatory Network); Member of Advisory/Expert Panel of MIMOS (Malaysia Institute of Microsystems); Steering Committee Member, ISC (International Supercomputing Conference)

Fourth author: Guoqun zhao

Education:

1988-1991 Ph.D: Department of Materials Engineering, Shanghai Jiaotong University, China
1983-1986 M.S. Department of Materials, Shandong University, China
1979-1983 B.S. Department of the second Mechanical Engineering, Shandong University, China

Research area:

Plastic forming theory and technology, mold design and manufacture, numerical simulation of plastic forming, mold CAD/CAM/CAE, mold design and optimization, product/mold rapid design and manufacturing process

Working Experiences:

2006-Date Dean, professor, doctoral tutor, School of Materials Science and Engineering, Shandong University, China
2002-2005 Director, Department of Science and Technology, Shandong University
2001-2001 Senior visiting scholar, Department of Mechanics and Materials, Wright State University
1997-2001 Professor, doctoral tutor, director of mold center, Department of Materials Science and Engineering, Shandong University
1993-1997 Postdoctoral researcher, Department of Mechanics and Materials, Wright State University
1991-1993 Associate professor, Department of Materials Science, Shandong University

Achievements:

(1) Published 4 classics and manuals, and published more than 200 papers.
(2) Obtained more than 10 patents, register 3 kinds of software.

ISSN: 2277-3754
ISO 9001:2008 Certified
International Journal of Engineering and Innovative Technology (IJEIT)
Volume 3, Issue 3, September 2013

(3) Hosted more than 20 projects, containing the National Science and Technology Support Program, the National Outstanding Youth Foundation, the National Natural Science Foundation of China, the provincial (ministry) level research projects and enterprises commissioned project etc.

(4) Obtained the second prize of National Science and Technology Progress award in China. Obtained 18 types of provincial and ministerial level scientific and technological achievement awards.